MASTER COPY KEEP THIS COPY FOR REPRODUCTION PURPOSES

AD-A271 127

IMENTATION PAGE

Form Approved
OMB No. 0704-0188

2. REPORT DATE	3. REPORT TYPE AND DATES COVERED

4. TITLE AND SUBTITLE
Angular Intensity Correlations in the Double Passage of Waves through a Random Phase Screen

5. FUNDING NUMBERS
DAAL03-89-C-0036

(2)

6. AUTHOR(S)
Hector M. Escamilla, Eugenio R. Mendez, and David F. Hotz

7. PERFORMING ORGANIZATION NAME(S) AND ADDRESS(ES)
Surface Optics Corporation
P.O. Box 261602
San Diego, CA 92196-1602

93-24959

9. SPONSORING/MONITORING AGENCY NAME(S) AND ADDRESS(ES)
U. S. Army Research Office
P. O. Box 12211
Research Triangle Park, NC 27709-2211

10. SPONSORING/MONITORING AGENCY REPORT NUMBER
ARO 27031.23-GS

11. SUPPLEMENTARY NOTES
The view, opinions and/or findings contained in this report are those of the author(s) and should not be construed as an official Department of the Army position, policy, or decision, unless so designated by other documentation.

12a. DISTRIBUTION/AVAILABILITY STATEMENT
Approved for public release; distribution unlimited.

12b. DISTRIBUTION CODE

13. ABSTRACT *(Maximum 200 words)*

The problem of light scattering in folded-path or double-passage configurations is studied theoretically. Assuming as the random medium a deep phase screen that introduces Gaussian-distributed phase fluctuations, we study the motion of the speckle as the source is moved. Some attention is also given to the phenomenon of backscattering enhancement. Our analysis is based on a novel expression for the complex amplitude that has a simple physical interpretation. For simplicity, only the one-dimensional case is considered, but an extension of the analysis to two-dimensional screens is not difficult.

Using the factorization properties of the moments of a complex Gaussian process, we are able to derive analytical expressions for the mean intensity and the intensity correlation of the backscattered radiation. We find that, in most cases, the speckle field decorrelates rapidly as one moves the angle of incidence and shifts toward the direction of specular reflection with a rate of motion that is different from that of the angle of incidence. We also find conditions under which, when the angle of incidence is modified, the speckle pattern produced in the region of observation tracks the backscattering direction.

14. SUBJECT TERMS	15. NUMBER OF PAGES
Enhanced backscattering, double-passage analysis, speckle motion, multiple scattering, random phase screen	16. PRICE CODE

17. SECURITY CLASSIFICATION OF REPORT	18. SECURITY CLASSIFICATION OF THIS PAGE	19. SECURITY CLASSIFICATION OF ABSTRACT	20. LIMITATION OF ABSTRACT
UNCLASSIFIED	UNCLASSIFIED	UNCLASSIFIED	UL

a reprint from Applied Optics

Angular intensity correlations in the double passage of waves through a random phase screen

Héctor M. Escamilla, Eugenio R. Méndez, and David F. Hotz

The problem of light scattering in folded-path or double-passage configurations is studied theoretically. Assuming as the random medium a deep phase screen that introduces Gaussian distributed phase fluctuations, we study the motion of the speckle as the source is moved. Some attention is also given to the phenomenon of backscattering enhancement. Our analysis is based on a novel expression for the complex amplitude that has a simple physical interpretation. For simplicity, only the one-dimensional case is considered, but an extension of the analysis to two-dimensional screens is not difficult.

Using the factorization properties of the moments of a complex Gaussian process, we are able to derive analytical expressions for the mean intensity and the intensity correlation of the backscattered radiation. We find that, in most cases, the speckle field decorrelates rapidly as one moves the angle of incidence and shifts toward the direction of specular reflection with a rate of motion that is different from that of the angle of incidence. We also find conditions under which, when the angle of incidence is modified, the speckle pattern produced in the region of observation tracks the backscattering direction.

Key words: Enhanced backscattering, double-passage analysis, speckle motion, multiple scattering, random phase screen.

1. Introduction

The problem of light scattering in folded-path or double-passage configurations has been studied in the last three decades by several authors.[1–6] The system is known to exhibit the phenomenon of backscattering enhancement. This phenomenon can be explained by considering the coherent addition of waves that follow identical paths in opposite directions on interaction with the random medium. Most of these studies have dealt with the propagation through an extended random medium, and Ref. 6 provides several references for this case. More recently, the scattering system consisting of a plane mirror in the diffraction field of a deep random phase screen has also been studied by several authors.[4,5,7–10] To our knowledge, however, only the mean intensity and the first-order spatial coherence function of the scattered light have been studied.

In this paper we study theoretically the deep phase screen double-passage configuration [see Fig. 1(a)] with particular interest in the correlation of the intensity fluctuations that describes the motion of the speckle as the source is moved, but some attention is also given to the angular distribution of the mean intensity around the backscattering direction. Our analysis is based on an expression for the scattered complex amplitude that can be obtained by manipulating the diffraction integrals that describe the propagation to the observation point. Assuming that a Gaussian speckle pattern[11] is formed in the plane of the mirror and that the speckle grain on the mirror is much smaller than the mirror aperture, we derive exact (within the model) analytical expressions for the mean intensity and the intensity correlation of the backscattered radiation by using the factorization properties of the moments of a complex Gaussian process. In this paper we deal with a one-dimensional random phase screen that introduces smoothly varying Gaussian-distributed phase fluctuations, but the calculations can be easily extended to the case of two-dimensional phase screens.

We find that, under certain circumstances, when the angle of incidence is modified, the speckle pattern produced in the region of observation tracks the backscattering direction. This is in contrast with the well-known laws of speckle motion with random surfaces[12,13] and with the type of motion found for volume scatterers.[14–17] Another interesting feature present in our calculations is that, in some cases, the

The authors are with the División de Física Aplicada, Centro de Investigación Científica y de Educación Superior de Ensenada, Apartado Postal 2732, 22800 Ensenada, B. C. Mexico.

Received 29 May 1992.
0003-6935/93/152734-10$05.00/0.

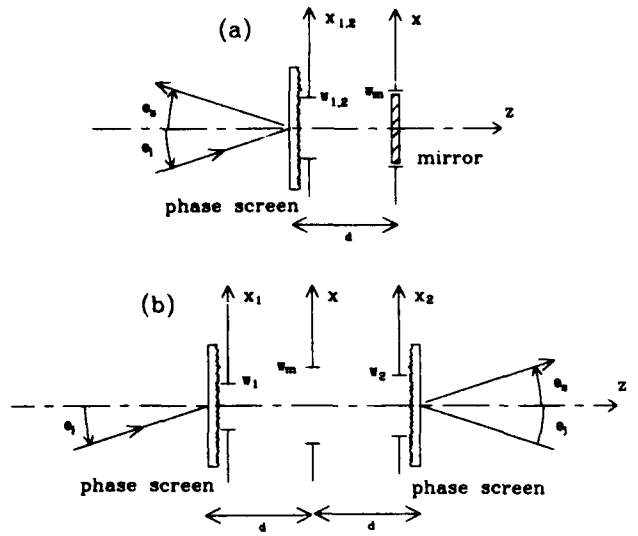

Fig. 1. Scattering geometry: (a) backscattering configuration, (b) equivalent unfolded geometry with two identical screens.

speckle pattern is nearly symmetric about the backscattering direction.

Using these results, we propose a modification of the original scattering geometry. With this new configuration, the backscattering enhancement, the symmetry of the speckle pattern, and the tracking of the speckle pattern of the backscattering direction are present under less restrictive conditions.

2. Formulation of the Problem

The double-passage configuration is shown in Fig. 1(a). A plane mirror lies in the Fresnel region of the phase screen. Finite apertures are located in the plane of the mirror and of the screen. The angles of incidence θ_i and of scattering θ_s are taken as positive in the sense indicated by the arrows in the figure. It is clear that the unfolded geometry of Fig. 1(b) is equivalent to that shown in Fig. 1(a). The aperture W_1 refers to the width of the incoming beam.

A. Scattered Complex Amplitude

With reference to Fig. 1(b), we see that a nearly collimated monochromatic Gaussian beam of $1/e$ amplitude radius W_1 is incident upon the first phase screen, which is located on the plane x_1, at an angle θ_i with respect to the z axis. This incident complex amplitude $A_i(x_1)$ may we written as

$$A_i(x_1) = K_0 \exp(-ikx_1 \sin\theta_i)\exp\left(-\frac{x_1^2}{W_1^2}\right), \quad (1)$$

where K_0 is a complex constant and $k = 2\pi/\lambda$, λ being the wavelength of the incident light. The complex amplitude of the scattered light in the plane of the mirror, which is denoted by $A(x, \theta_i)$, can be found by using the Kirchhoff diffraction theory in the Fresnel approximation. We have

$$A(x, \theta_i) = K_1 \int_{-\infty}^{\infty} A_i(x_1)\exp[i\phi(x_1)]\exp\left[\frac{ik}{2d}(x_1 - x)^2\right]dx_1, \quad (2)$$

where $\phi(x_1)$ is the random phase introduced by the screen, d is the distance from the screen to the mirror, and K_1 is another complex constant. The aperture function in the mirror plane is given by

$$T_0(x) = \exp\left(-\frac{x^2}{W_m^2}\right), \quad (3)$$

where W_m is the aperture radius at the $1/e$ point. The complex amplitude $A(x_2)$, which is incident upon the second phase screen located in the plane x_2, can be written as

$$A(x_2) = K_2 \int_{-\infty}^{\infty} A(x, \theta_i)T_0(x)\exp\left[\frac{ik}{2d}(x_2 - x)^2\right]dx, \quad (4)$$

where K_2 is a complex constant, and we have again made use of the Fresnel approximation. At an observation point in the far field of the second screen, the scattered complex amplitude can be written as

$$A(\theta_i, \theta_s) = K \int_{-\infty}^{\infty} A(x_2)\exp\left(-\frac{x_2^2}{W_2^2}\right) \times \exp[i\phi(x_2)]\exp(-ikx_2 \sin\theta_s)dx_2, \quad (5)$$

where θ_s denotes the direction of observation and K is another complex constant; we have included a Gaussian aperture function of radius W_2 in the plane of the second screen. From Eqs. (3)–(5) we may write, after interchanging the orders of integration,

$$A(\theta_i, \theta_s) = K \int_{-\infty}^{\infty} \exp\left(-\frac{x^2}{W_m^2}\right)A(x, \theta_i)A(x, \theta_s)dx, \quad (6)$$

where

$$A(x, \theta_s) = K_2 \int_{-\infty}^{\infty} \exp\left(-\frac{x_2^2}{W_2^2}\right)\exp[i\phi(x_2)] \times \exp\left[\frac{ik}{2d}(x_2 - x)^2\right]\exp(-ikx_2 \sin\theta_s)dx_2. \quad (7)$$

The quantity $A(x, \theta_s)$ is the complex amplitude that a point source located at the observation point in the far field would produce in the plane of the mirror. Substitution of Eq. (1) into Eq. (2) shows that, except for an irrelevant constant factor, Eqs. (2) and (7) have exactly the same form. Our approach is based on Eq. (6) and a few additional assumptions that are described in Subsection 2.B. Equation (6) has a simple physical interpretation: mathematically it is the product of two speckle patterns integrated over

the mirror aperture. This expression has some close parallels with the equation describing image formation in confocal scanning microscopy.[18]

B. Correlation of the Scattered Intensity

At this point it is necessary to introduce a statistical model for the phase fluctuations $\phi(x)$. We assume that $\phi(x)$ is a stationary zero-mean Gaussian random process with a Gaussian correlation coefficient $\rho(x - x')$;

$$\rho(x - x') = \frac{\langle \phi(x)\phi(x') \rangle}{\sigma^2} = \exp\left(- \frac{|x - x'|^2}{\xi^2} \right), \quad (8)$$

where σ^2 is the variance of the random phase fluctuations and ξ is the characteristic correlaton length of the process.

Now, for a deep phase screen, $\sigma^2 \gg 1$, and if, in addition, $W_1^2 \gg \xi^2$ and $(k\xi^2/2d) \ll 1$, then the complex amplitude $A(x, \theta_i)$ corresponds to that of a fully developed speckle pattern.[4,11] That is, $A(x, \theta_i)$ is a zero-mean circular complex Gaussian random variable (CCGRV).[11] The condition $(k\xi^2/2d) \ll 1$ ensures that the mirror is far from the focusing region of the screen where strong departures from Gaussian statistics take place.[19] Likewise, if $W_2^2 \gg \xi^2$, $A(x, \theta_s)$ is also a zero-mean CCGRV. In addition, if W_m is much greater than the speckle size in the plane of the mirror, the scattered complex amplitude $A(\theta_i, \theta_s)$ is also a zero-mean CCGRV.

Consider now the intensity $I(\theta_i, \theta_s)$ at detection angle θ_s, which is due to an incoming beam incident at angle θ_i, and the intensity $I(\theta_i', \theta_s')$ at detection angle θ_s', which is due to an incoming beam at incident angle θ_i'. With the statements made above regarding the statistics of $A(\theta_i, \theta_s)$, the intensity correlation $C_I(\theta_i, \theta_s; \theta_i', \theta_s') = \langle I(\theta_i, \theta_s) I(\theta_i', \theta_s') \rangle$ can be written as[20]:

$$C_I(\theta_i, \theta_s; \theta_i', \theta_s') = \langle I(\theta_i, \theta_s) \rangle \langle I(\theta_i', \theta_s') \rangle + |C_A(\theta_i, \theta_s; \theta_i', \theta_s')|^2, \quad (9)$$

where

$$C_A(\theta_i, \theta_s; \theta_i', \theta_s') = \langle A(\theta_i, \theta_s) A^*(\theta_i', \theta_s') \rangle. \quad (10)$$

Using Eq. (6), we see that the problem reduces to the calculation of the function:

$$C_A(\theta_i, \theta_s; \theta_i', \theta_s') = |K|^2 \int_{-\infty}^{\infty} \int_{-\infty}^{\infty} \exp\left(- \frac{x^2 + x'^2}{W_m^2} \right) \times \langle A(x, \theta_i) A(x, \theta_s) A^*(x', \theta_i') A^*(x', \theta_s') \rangle dx dx'. \quad (11)$$

Recalling again the statistical considerations made above, we also find that the fourth-order moment in the integrand of Eq. (11) can be expressed as a sum of products of first-order correlation functions.[20] Thus we can write

$$C_A(\theta_i, \theta_s; \theta_i', \theta_s') = C_1(\theta_i, \theta_s; \theta_i', \theta_s') + C_2(\theta_i, \theta_s; \theta_i', \theta_s'), \quad (12)$$

where

$$C_1(\theta_i, \theta_\varepsilon; \theta_i', \theta_s') = |K|^2 \int_{-\infty}^{\infty} \int_{-\infty}^{\infty} \exp\left(- \frac{x^2 + x'^2}{W_m^2} \right) \langle A(x, \theta_i) A^*(x', \theta_i') \rangle \times \langle A(x, \theta_s) A^*(x', \theta_s') \rangle dx dx', \quad (13)$$

and

$$C_2(\theta_i, \theta_s; \theta_i', \theta_s') = |K|^2 \int_{-\infty}^{\infty} \int_{-\infty}^{\infty} \exp\left(- \frac{x^2 + x'^2}{W_m^2} \right) \langle A(x, \theta_i) A^*(x', \theta_s') \rangle \times \langle A(x, \theta_s) A^*(x', \theta_i') \rangle dx dx', \quad (14)$$

The last two expressions involve only the calculation of second-order moments or correlations of the field amplitude, and are much simpler to calculate than the fourth-order moment of Eq. (11). The amplitude correlations in Eqs. (13) and (14) were evaluated in the limit $\sigma^2 \gg 1$ by using a steepest-descents method (see Appendix A). Using these results, we can obtain analytical expressions for $C_1(\theta_i, \theta_s; \theta_i', \theta_s')$ and $C_2(\theta_i, \theta_s; \theta_i', \theta_s')$ without further approximations. The result involves some rather long algebraic expressions that are difficult to reduce and thus are given in Appendix A. A simple formula for a particular case is given in Section 3.

The mean intensity is then calculated from

$$\langle I(\theta_i, \theta_s) \rangle = C_A(\theta_i, \theta_s; \theta_i, \theta_s), \quad (15)$$

while the normalized intensity correlation $\gamma_i(\theta_i, \theta_s; \theta_i', \theta_s')$ is given by

$$\gamma_i(\theta_i, \theta_s; \theta_i', \theta_s') = 1 + |\gamma_A(\theta_i, \theta_s; \theta_i', \theta_s')|^2 = 1 + \frac{|C_A(\theta_i, \theta_s; \theta_i', \theta_s')|^2}{C_A(\theta_i, \theta_s; \theta_i, \theta_s) C_A(\theta_i', \theta_s'; \theta_i', \theta_s')}. \quad (16)$$

It is pertinent to mention that, recently, a compact formula for the mean intensity produced by the scattering of a Gaussian beam by the double passage through a deep phase screen has been derived that also uses the factorization properties of the moments of a Gaussian random process.[10]

3. Results

We now turn our attention to the study of the behavior of the angular distribution of the mean intensity around the backscattering direction. Figure 2 shows the evolution of the enhancement factor E_f as the distance d from the phase screen to the

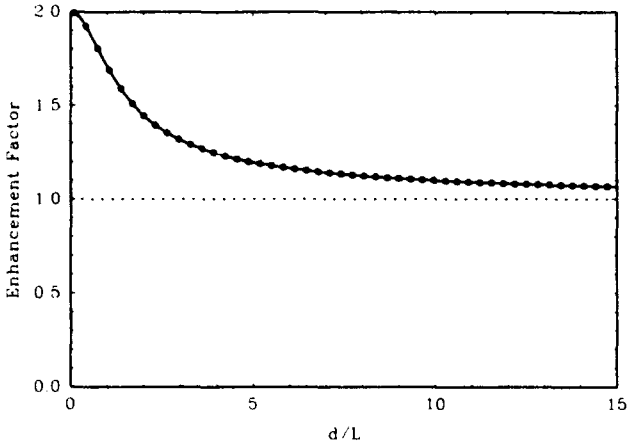

Fig. 2. Enhancement factor E_f as a function of the normalized distance d/L between the mirror and the phase screen. For the numerical calculations W_2 and W_m were assumed to be infinite, L = 6.206 mm (see text) and θ_i = 5 mrad.

mirror increases for the case of infinite apertures at the mirror and the second screen. We define the enhancement factor E_f as the ratio of the mean intensity in the backscattering direction to the mean background intensity. In Fig. 2, the circles represent the values obtained from the evaluation of the general formulas given in Appendix A, while the solid curve is a plot of the expression

$$E_f = 1 + \frac{1}{[1 + (d/L)^2]^{1.2}}, \tag{17}$$

where the normalization distance L is given by

$$L = \frac{k\xi W_1}{2\sigma}. \tag{18}$$

For the numerical calculations presented we have set λ = 0.6328 μm, σ = 8 rad, ξ = 5.0 μm, and W_1 = 2 mm. So the parameter L was fixed at the value L = 6.206 mm. Equation (17) can be derived from the results given in Ref. 4. The agreement between the two plots is excellent. It is seen that the height of the peak diminishes as the screen to the mirror distance increases. This is because, as this distance increases, more of the scattered light reflected by the mirror onto the screen lies outside the region illuminated in the first passage. It is only the region of overlap that contributes to the backscattering enhancement. The light reflected outside this region contributes to only the background scattered intensity.

The relative enhancement can also be increased by reducing the area of the screen illuminated in the second passage by placing a physical aperture at either the mirror or at the screen. This is illustrated in Fig. 3 for a normalized distance d/L = 6.5, for which expression (17) predicts a small enhancement (see Fig. 2). In Fig. 3(a) the aperture radius of the mirror has been set to one half of the radius of the incoming Gaussian beam. A high value is obtained

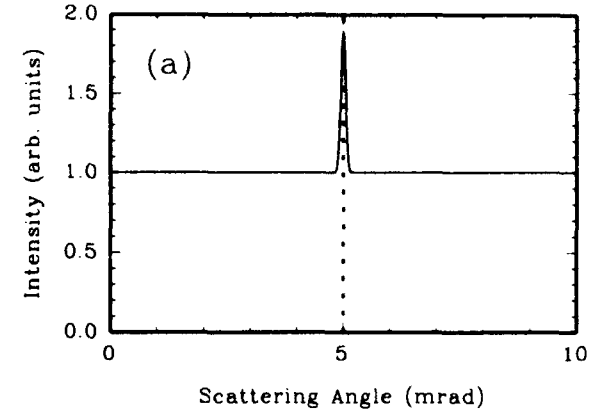

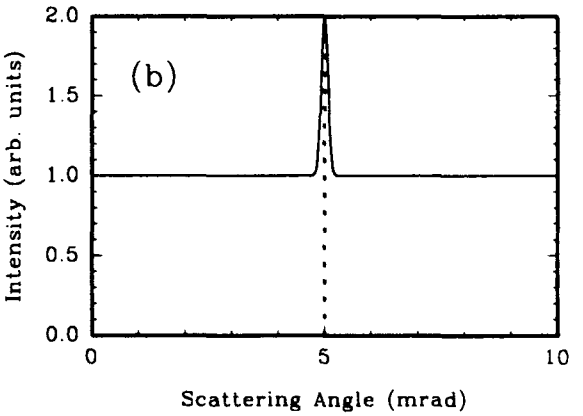

Fig. 3. Angular distribution of mean intensity as a function of the scattering angle θ_s for the cases of reduced apertures at the mirror or phase screen. The dots indicate the direction of incidence θ_i = 5 mrad. Here d = 6.5 L and (a) $W_m = W_1/2$ and W_2 infinite, (b) $W_2 = W_1$ and W_m infinite.

for the relative enhancement because, after reflection, the illuminated region of the second screen almost coincides with the area illuminated in the first passage. Figure 3(b), on the other hand, shows that the maximum theoretical enhancement factor of 2 (see Refs. 21–23) is achieved when the apertures at the two screens have equal sizes, as this maximizes the proportion of reversible paths. The mirror, in this case, has been assumed to be infinite.

In Fig. 4 we study the motion of the speckle pattern as the direction of the incoming beam changes. We proceed by first fixing the original angles of incidence θ_i and detection θ_s. We then choose a new angle of incidence θ_i' and find the maximum value of the correlation $\gamma_i(\theta_i, \theta_s; \theta_i', \theta_s')$ as we scan the second angle of observation θ_s'. In these figures, the vertical dashed–dotted line indicates the original direction of observation θ_s while the dotted line indicates the original direction of incidence θ_i. Figure 4(a) is a plot of the maximum value of the intensity correlation

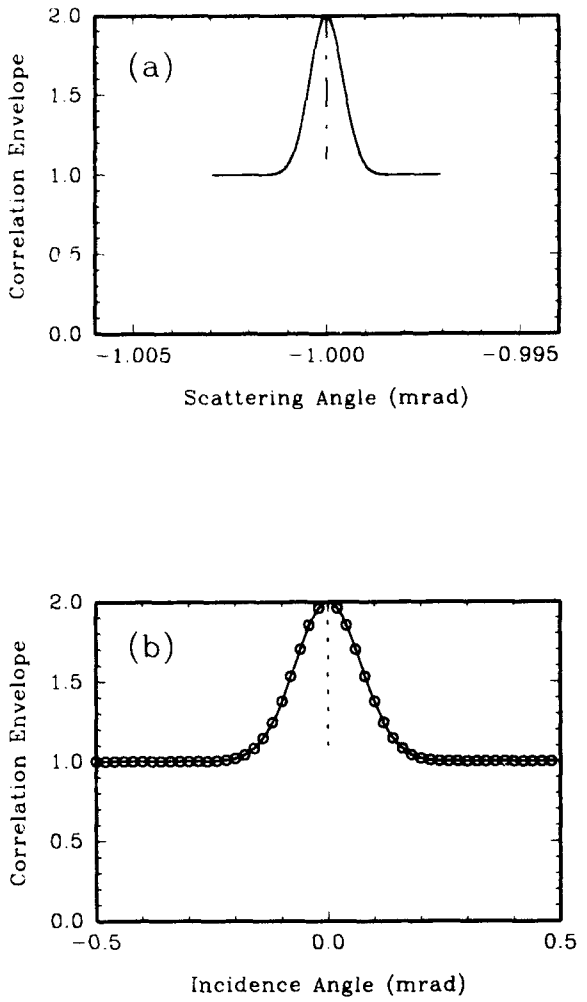

Fig. 4. Envelopes of the intensity correlation functions. The dashed–dotted vertical line in (a) indicates the original direction of observation, while the dotted line in (b) indicates the original direction of incidence. Here $d = 6.5\ L$, $W_1 = W_2$, W_m is infinite, $\theta_i = 0$ mrad and $\theta_s = -1$ mrad. (a) Maximum values of the intensity correlation function as a function of the scattering angle θ_s', (b) maximum values of the intensity correlation function as a function of the angle of incidence θ_i' (circles) and angular distribution of mean intensity with $\theta_s' = 0$ mrad as a function of the angle of incidence θ_i' (solid curve).

function as a function of the angle of observation θ_s' at which the maximum occurs for each new angle of incidence θ_i'; the curve represents, then, the intensity correlation envelope. It should be pointed out, however, that, in general, the ratio of the angular shift of the speckle pattern to the angular shift in the angle of incidence is not equal to 1. This ratio depends on the geometry and, in particular, it depends on the distance d. To illustrate the fact that the speckle does not move at the same rate as the angle of incidence, we show in Fig. 4(b) a plot of the correlation envelope shown in Fig. 4(a) in terms of the direction of incidence θ_i'. The correlation envelope shown in Fig. 4(b) then represents (for given angles θ_i, θ_s, and θ_i') the maximum correlation obtained by scanning the angle of scattering θ_s' plotted as a function of the angle of incidence θ_i'. It can be seen from Fig. 4(a) that, for the distance $d = 6.5\ L$ employed in the figure, the full width of the correlation envelope, as a function of the scattering angle θ_s', equals approximately 2 μrad. This width corresponds to an interval of angles of incidence θ_i' of approximately 3 mrad, as can be seen from the curve plotted in Fig. 4(b). This indicates that, in the situation considered, the speckle pattern is practically static, and decorrelates as the angle of incidence is changed. The solid curve in Fig. 4(b) represents the mean intensity for $\theta_s' = 0$ mrad (which corresponds to the original angle of incidence θ_i) plotted as a function of the angle of incidence θ_i'. Invoking reciprocity arguments we can see that the same curve would be obtained by setting $\theta_i = 0$ mrad and plotting $\langle I(\theta_i, \theta_s)\rangle$ as a function of θ_s. The solid curve in Fig. 4(b) represents, then, the backscattering enhancement peak, and it is remarkable that the two curves plotted in this figure are practically the same. A similar result holds for scattering from dense media, where it has been shown that the shape of the envelope of the correlation is equal to the square of the backscattering enhancement peak.[24] We also mention that the situation shown in Fig. 4(b) does not always hold. For instance, if the mirror is moved closer to the phase screen, one eventually reaches a point beyond which the shape of the envelope correlation and that of the backscattering peak are different.

Figure 5 shows two aspects of the behavior of the intensity correlation function as the direction of incidence changes from θ_i to θ_i'. The geometry of the arrangement is the same as in Fig. 4, but we have now set the distance $d = 0.8\ L$. Also, as in Fig. 4, the vertical dashed–dotted line in the upper half of these figures indicates the original direction of observation θ_s, while the dotted lines indicate the original direction of incidence θ_i. The long-dashed vertical lines in the bottom halves of the figures indicate the new direction of incidence θ_i', while the solid-vertical lines indicate the new direction of observation θ_s' for which maximum correlation is achieved. In Fig. 5(a), the thick solid curve corresponds to the intensity correlation function, while the thin curve shows the envelope of the intensity correlation function. For the value of d/L employed in Fig. 5(a), the envelope is much wider than that in Fig. 4(a). We also see from Fig. 5(a) that, as the direction of incidence changes from $\theta_i = 0.0$ mrad to $\theta_i' = 0.15$ mrad, the peak of the intensity correlation function, and thus the speckle pattern, moves in the direction of the specular reflection from the original angle of observation $\theta_s = -1$ mrad to the position $\theta_s' = -1.04$ mrad. In Fig. 5(b), the original directions of incidence and observation are, respectively, $\theta_i = 0.0$ mrad and $\theta_s = -1.0$ mrad. It can be seen that, when the new direction of incidence θ_i' coincides with the original direction of observation θ_s, the peak of the intensity correlation function appears at the original direction of incidence

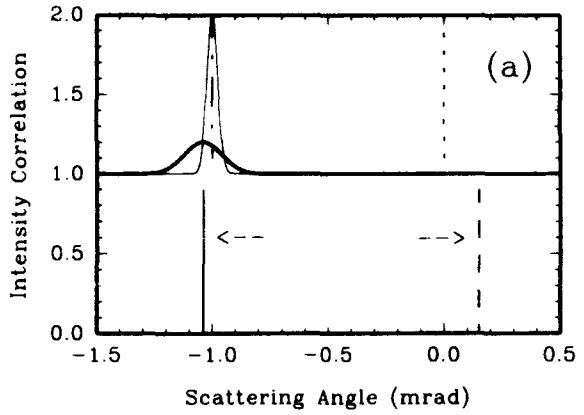

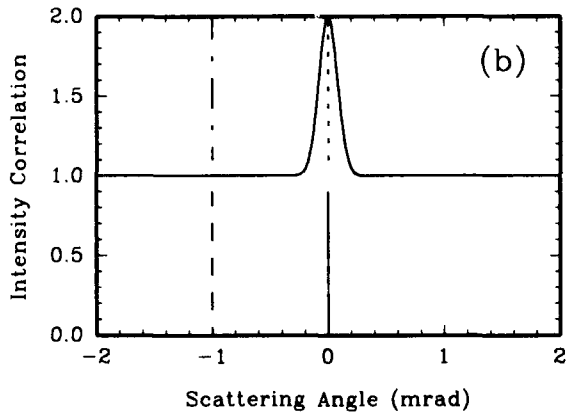

Fig. 5. Shift of the intensity correlation peak with a change in the angle of incidence. The abscissas correspond to the scattering angle θ_s'. The dashed–dotted vertical line indicates the original direction of observation, while the dots indicate the original direction of incidence. The long-dashed vertical line indicates the new direction of incidence while the solid vertical line indicates the angle of observation for which maximum correlation occurs. Here $d = 0.8\,L$, $W_1 = W_2$, W_m is infinite, $\theta_i = 0$ mrad, and $\theta_s = -1$ mrad. (a) Intensity correlation function for $\theta_i' = 0.15$ mrad (thick curve) and envelope of the intensity correlation function (thin curve). The maximum correlation occurs at $\theta_s = -1.04$ mrad. (b) Intensity correlation function for $\theta_i' = \theta_s$.

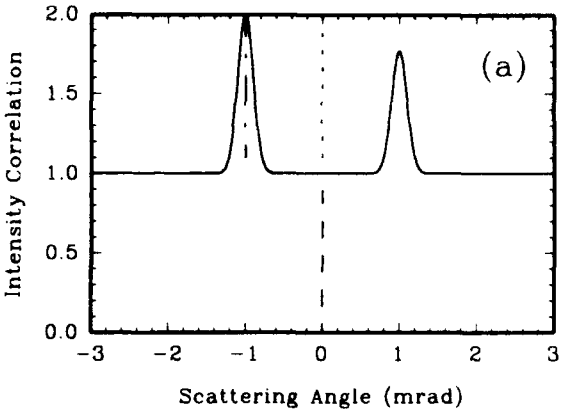

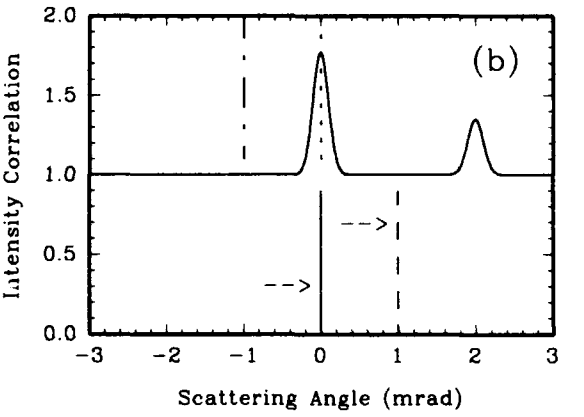

Fig. 6. Intensity correlation functions as functions of the scattering angle θ_s' for a small mirror aperture. The vertical lines have the same meaning as in Fig. 5. Here $d = L$, $W_m = 0.025\,W_1$, W_2 is infinite, $\theta_i = 0$ mrad, and $\theta_s = -1$ mrad. (a) Intensity correlation for $\theta_i' = \theta_i$ (spatial autocorrelation), (b) intensity correlation function for $\theta_i' = 1.0$ mrad.

θ_i. So, when source and detector are interchanged, the corresponding intensities are perfectly correlated. This result shows that the formulas derived in Appendix A obey reciprocity. This kind of correlation was recently discussed for volume scatterers and has been termed the "time-reversed memory effect."[17]

In Fig. 6 we consider the case of a small aperture at the mirror, much smaller than the cross section of the incoming beam. For these figures we assumed an infinitely large aperture at the second screen. Figure 6(a) shows the spatial intensity autocorrelation function. It can be seen that the speckle pattern is nearly symmetrical with respect to the backscattering direction. This is because [with reference to Fig. 1(b)] the light scattered from the first screen that reaches the second screen goes through a small aperture on the axis of the system so that an inverted image of the area illuminated on the first screen is projected onto the second. Figure 6(b) shows that when the incident direction changes from $\theta_i = 0$ to $\theta_i' = 1$ mrad, the correlation peaks move in a direction opposite to that of the specular direction and at the same rate as the incident direction. That is, in this case, the speckle pattern tracks the backscattering direction.

These striking results are due to the fact that, for the complex amplitudes $A(x, \theta_i)$ and $A(x, \theta_s)$ [see Eq. (6)], the phase curvatures within the mirror aperture are negligible. This suggests a modification of the scattering geometery that will produce these effects under less restrictive conditions. The new geometry is shown in Fig. 7. The simple formula referred to in

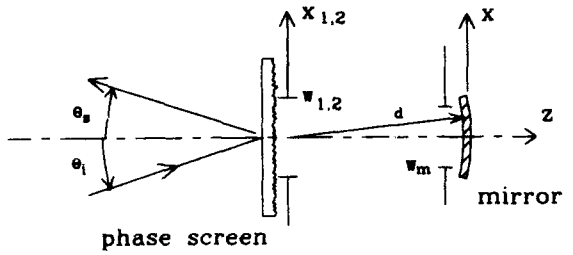

Fig. 7. Double-passage configuration with the phase screen at the center of curvature of a spherical mirror.

Subsection 2.B was derived for the case $W_1 = W_2 = W$ and for this specialized geometry, including a spherical mirror, with an aperture of radius W_m, situated in the far field of the screen. The radius of curvature of the mirror is d and is equal to the distance from the screen to the mirror.

It is found that up to a constant factor, the amplitude correlation is given by the expression

$$\gamma_A(\theta_i, \theta_s; \theta_i', \theta_s') = \exp\left[-\frac{1}{8}\frac{(\theta_i^+ + \theta_s^+)^2}{\varphi_m^2 + \varphi_e^2} - \frac{1}{8}\frac{(\theta_i^- + \theta_s^-)^2}{\varphi_m^2}\right] \times \left\{\exp\left[-\frac{1}{8}\frac{(\theta_i^+ - \theta_s^+)^2}{\varphi_e^2} - \frac{1}{4}\frac{(\theta_i^- - \theta_s^-)^2}{\varphi_s^2}\right] + \exp\left[-\frac{1}{8}\frac{(\theta_i^- - \theta_s^-)^2}{\varphi_e^2} - \frac{1}{4}\frac{(\theta_i^+ - \theta_s^+)^2}{\varphi_s^2}\right]\right\}, \quad (19)$$

where

$$\theta_i^+ = \sin\theta_i + \sin\theta_i', \quad (20)$$

$$\theta_i^- = \sin\theta_i - \sin\theta_i', \quad (21)$$

$$\theta_s^+ = \sin\theta_s + \sin\theta_s', \quad (22)$$

$$\theta_s^- = \sin\theta_s - \sin\theta_s', \quad (23)$$

$$\varphi_s = \frac{2}{kW}, \quad (24)$$

$$\varphi_e = \frac{2\sigma}{k\xi}, \quad (25)$$

$$\varphi_m = \frac{W_m}{d}. \quad (26)$$

These last three quantities represent, respectively, the angular widths of the speckle, of the speckle envelope, and of the mirror. To derive expression (19) we assumed that $\varphi_e, \varphi_m \gg \varphi_s$.

Also, it is straightforward to show that, with approximations consistent with those employed in the derivation of Eq. (19), the mean intensity predicted by this equation is given by

$$\langle I(\theta_i, \theta_s)\rangle = \exp\left\{-\frac{1}{2\varphi_e^2}\left[\frac{\varphi_e^2}{\varphi_e^2 + \varphi_m^2}(\sin\theta_i + \sin\theta_s)^2 + (\sin\theta_i - \sin\theta_s)^2\right]\right\} \times \left\{1 + \exp\left[-\frac{(\sin\theta_i - \sin\theta_s)^2}{\varphi_s^2}\right]\right\}. \quad (27)$$

which predicts a broad envelope with a narrow peak (width φ_s) in the backscattering direction ($\theta_s = \theta_i$).

Figure 8 corresponds to the geometry depicted in Fig. 7, in which the phase screen is at the center of curvature of the spherical mirror. Figure 8(a) shows the behavior of the mean intensity. It is seen that the relative value of the backscattering enhancement reaches a value of 2. The reason for this is that, in the present case, an image of the region of the screen

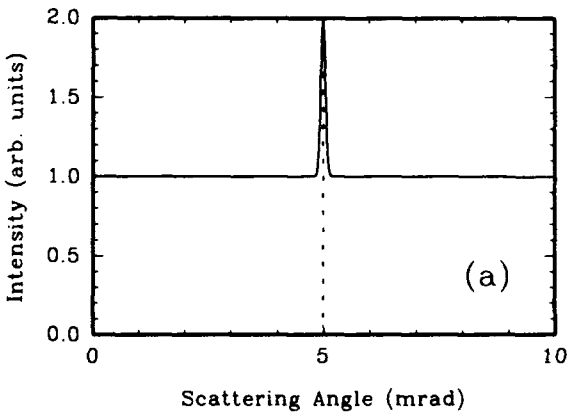

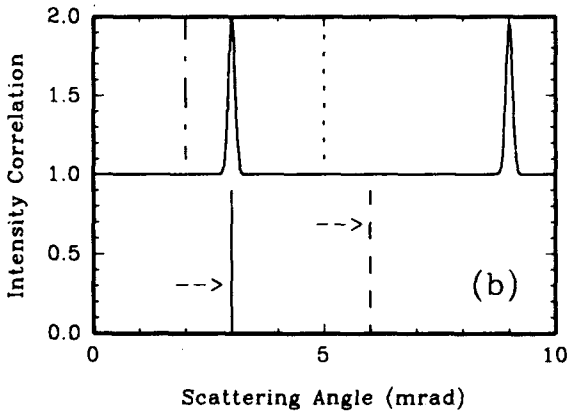

Fig. 8. Mean intensity and intensity correlation for the geometry shown in Fig. 7. The vertical lines have the same meaning as in Fig. 5. The relevant parameters are $d = 80.0\,L$, $W_m = 5\,W_1$, W_2 is infinite, and $\theta_i = 5$ mrad. (a) Angular distribution of mean intensity as a function of θ_s, (b) intensity correlation plotted as a function of the scattering angle θ_s', with $\theta_s = 2$ mrad and $\theta_i' = 6$ mrad.

illuminated by the incoming beam is formed on the screen by the mirror. This image is inverted and is of unit magnification. The intensity correlation function in Fig. 8(b) shows the same features observed in Fig. 6. The autocorrelation function shows two peaks, indicating the symmetry of the speckle pattern with respect to the backscattering direction. Also, as the angle of incidence of the incoming beam is changed, the speckle pattern tracks the backscattering direction and not the specular direction, as would be the case with a single-scattering rough surface. These features can be explained from Eq. (19): The term $(\theta_i^- - \theta_s^-)$ in this equation is the one responsible for the tracking of the backscattering direction, as it predicts a peak when $\sin \theta_s' = \sin \theta_i' + (\sin \theta_s - \sin \theta_i)$. On the other hand, the term $(\theta_i^+ - \theta_s^+)$ is responsible for the symmetry of the speckle pattern about the backscattering direction (i.e., $\theta_s' = \theta_i'$), as it predicts a peak when $\sin \theta_s' = \sin \theta_i' - (\sin \theta_s - \sin \theta_i)$.

4. Summary and Conclusions

We have studied the scattering of light resulting from double passage through a deep random phase screen for an incoming Gaussian beam. Our analysis is for a one-dimensional random phase screen but the extension to two dimensions is straightforward. Assuming that the complex amplitude of the speckle formed on the mirror follows Gaussian statistics, and that the speckle grain on the mirror is much smaller than the mirror aperture, we have derived formulas for the mean intensity of the backscattered light and for the correlation of the intensities for different directions of incidence and observation. Using the factorization properties of the moments of a complex Gaussian process, we have derived exact (within the model) analytical expressions for these two quantities. The formulas so obtained are long and difficult to interpret but we have studied a variety of double-passage configurations from the numerical evaluation of these expressions.

We have studied the backscattering enhancement factor as well as the motion of the speckle pattern as the angle of incidence is changed. We have found that, in general, the rate of change in the position of the speckle pattern is not the same as that of the angle of incidence. In normal circumstances, the speckle moves in the direction of the specular reflection at a rate slower than that of the incident beam and decorrelates with an envelope described approximately by the shape of the backscattering enhancement peak. Conditions have also been found under which the speckle pattern is symmetric about the backscattering direction and tracks the backscattering direction as the source is moved. The conditions for the observation of this effect are, however, fairly restrictive. The new geometry proposed, with a spherical mirror, exhibits enhanced backscattering, the symmetry of the speckle pattern, and the tracking of the backscattering direction under less restrictive conditions.

Appendix A

Apart from some constant factors, the amplitude correlations appearing in Eqs. (13) and (14) are of the general form

$$\langle A(x,\theta)A^*(x',\theta')\rangle = \int_{-\infty}^{\infty}\int_{-\infty}^{\infty} \exp\left[-\left(\frac{x_i^2}{W_i^2}+\frac{x_j^2}{W_j^2}\right)\right]\langle \exp[i\phi(x_i)]\exp[-i\phi(x_j)]\rangle \times \exp\left\{\frac{ik}{2d}[(x_i-x)^2-(x_j-x)^2]\right\} \times \exp[-ik(x_i\sin\theta - x_j\sin\theta')]dx_i dx_j. \quad \text{(A1)}$$

The steepest-descent method[10,25] that we employed for the calculation of these expressions basically consists of making the approximation

$$\langle \exp[i\phi(x)]\exp[-i\phi(x')]\rangle = \exp\{-\sigma^2[1-\rho(x-x')]\} \approx \exp\left(-\sigma^2\frac{|x-x'|^2}{\xi^2}\right) \quad \text{(A2)}$$

in the evaluation of the amplitude correlations given by Eq. (A.1). Using these results, we find that Eq. (13) gives

$$C_1(\theta_i,\theta_s;\theta_i',\theta_s') = |K|^2\frac{\pi^3 4d^2}{k^2}\frac{1}{(A_1A_2R)^{1/2}}\exp(X-B), \quad \text{(A3)}$$

where

$$X = \frac{k^2}{4}\frac{1}{R}\left\{Z\epsilon^2 + 2\frac{\sigma^2}{\xi^2}\left(\frac{1}{A_1}+\frac{1}{A_2}\right)\eta\epsilon + Z^*\eta^2\right\}, \quad \text{(A4)}$$

$$B = \frac{k^2}{4}\frac{1}{A_1}\left(z_1\sin^2\theta_i + z_1^*\sin^2\theta_i' - 2\frac{\sigma^2}{\xi^2}\sin\theta_i\sin\theta_i'\right) + \frac{k^2}{4}\frac{1}{A_2}\left(z_2\sin^2\theta_s + z_2^*\sin^2\theta_s' - 2\frac{\sigma^2}{\xi^2}\sin\theta_s\sin\theta_s'\right), \quad \text{(A5)}$$

$$R = |Z|^2 - \frac{\sigma^4}{\xi^4}\left(\frac{1}{A_1}+\frac{1}{A_2}\right)^2, \quad \text{(A6)}$$

$$A_1 = |z_1|^2 - \frac{\sigma^4}{\xi^4}, \quad \text{(A7)}$$

$$A_2 = |z_2|^2 - \frac{\sigma^4}{\xi^4}, \quad \text{(A8)}$$

with

$$\eta = \frac{1}{A_1}\left(z_1\sin\theta_i - \frac{\sigma^2}{\xi^2}\sin\theta_i'\right) + \frac{1}{A_2}\left(z_2\sin\theta_s - \frac{\sigma^2}{\xi^2}\sin\theta_s'\right), \quad \text{(A9)}$$

$$\epsilon = \frac{1}{A_1}\left(z_1^* \sin\theta_i' - \frac{\sigma^2}{\xi^2}\sin\theta_i\right) + \frac{1}{A_2}\left(z_2^* \sin\theta_s' - \frac{\sigma^2}{\xi^2}\sin\theta_s\right), \quad \text{(A10)}$$

$$Z = \frac{z_1}{A_1} + \frac{z_2}{A_2} + \frac{4d^2}{k^2}\left(\frac{1}{W_m^2} - i\frac{k}{d}\right), \quad \text{(A11)}$$

$$z_1 = \frac{1}{W_1^2} + \frac{\sigma^2}{\xi^2} + i\frac{k}{2d}, \quad \text{(A12)}$$

$$z_2 = \frac{1}{W_2^2} + \frac{\sigma^2}{\xi^2} + i\frac{k}{2d}. \quad \text{(A13)}$$

Similarly, it is found that Eq. (14) gives the following result:

$$C_2(\theta_i, \theta_s; \theta_i', \theta_s') = |K|^2 \frac{\pi^3 4d^2}{k^2}\frac{1}{|A|}\frac{1}{D^{1/2}}\exp(Y - V), \quad \text{(A14)}$$

where

$$Y = \frac{k^2}{4}\frac{1}{D}\left[S\nu^2 + 2\frac{\sigma^2}{\xi^2}\left(\frac{1}{A} + \frac{1}{A^*}\right)\mu\nu + S^*\mu^2\right], \quad \text{(A15)}$$

$$V = \frac{k^2}{4}\frac{1}{A}\left(z_1 \sin^2\theta_s + z_2^* \sin^2\theta_i' - 2\frac{\sigma^2}{\xi^2}\sin\theta_s \sin\theta_i'\right) + \frac{k^2}{4}\frac{1}{A^*}\left(z_2 \sin^2\theta_i + z_1^* \sin^2\theta_s' - 2\frac{\sigma^2}{\xi^2}\sin\theta_i \sin\theta_s'\right), \quad \text{(A16)}$$

$$D = |S|^2 - \frac{\sigma^4}{\xi^4}\left(\frac{1}{A} + \frac{1}{A^*}\right)^2, \quad \text{(A17)}$$

$$A = z_1 z_2^* - \frac{\sigma^4}{\xi^4}, \quad \text{(A18)}$$

with

$$\mu = \frac{1}{A}\left(z_1 \sin\theta_s - \frac{\sigma^2}{\xi^2}\sin\theta_i'\right) + \frac{1}{A^*}\left(z_2 \sin\theta_i - \frac{\sigma^2}{\xi^2}\sin\theta_s'\right), \quad \text{(A19)}$$

$$\nu = \frac{1}{A}\left(z_2^* \sin\theta_i' - \frac{\sigma^2}{\xi^2}\sin\theta_s\right) + \frac{1}{A^*}\left(z_1^* \sin\theta_s' - \frac{\sigma^2}{\xi^2}\sin\theta_i\right), \quad \text{(A20)}$$

$$S = \frac{z_1}{A} + \frac{z_2}{A^*} + \frac{4d^2}{k^2}\left(\frac{1}{W_m^2} - i\frac{k}{d}\right). \quad \text{(A21)}$$

The expressions corresponding to the geometry depicted in Fig. 7 are obtained by dropping the imaginary terms inside parentheses in Eqs. (A11) and (A21). Equation (19) was obtained by dropping, in addition, the imaginary terms in Eqs. (A12) and (A13) and by putting $W_1 = W_2 = W$.

This work has been supported by an internal grant from the Centro de Investigación Científica y de Educación Superior de Ensenada and by the U.S. Army Research Office under grant DAAL03-89-C-0036.

References

1. N. G. Denisov, "On wave scattering under full reflection conditions," Radiophys. Quantum Electron. **7**, 378–380 (1964).
2. A. G. Vinogradov, Yu. A. Kravstov, and V. I. Tatarskii, "The effect of intensification of backscattering by bodies placed in a medium with random inhomogeneities," Radiophys. Quantum Electron. **16**, 818–823 (1973).
3. Yu. A. Kravstov and A. I. Saichev, "Effects of double passage of waves in randomly inhomogeneous media," Sov. Phys. Usp. **25**, 494–508 (1982).
4. E. Jakeman, "Enhanced backscattering through a deep random phase screen," J. Opt. Soc. Am. A **5**, 1638–1648 (1988).
5. P. R. Tapster, A. R. Weeks and E. Jakeman, "Observation of backscattering enhancement through atmospheric phase screens," J. Opt. Soc. Am A **6**, 517–522 (1989).
6. R. Mazar and A. Bronshtein, "Double passage analysis in random media using two-scale random propagators," Waves Random Media **1**, 341–362 (1991).
7. E. Jakeman, P. R. Tapster, and A. R. Weeks, "Enhanced backscattering through a deep random phase screen," J. Phys. D **21**, 32–36 (1988).
8. G. Welch and R. Phillips, "Simulation of enhanced backscattering by a phase screen," J. Opt. Soc. Am. A **7**, 578–584 (1990).
9. B. S. Agrovskii, A. N. Bogaturov, A. S. Gurvich, S. V. Kireev, and V. A. Myakinin, "Enhanced backscattering from a plane mirror viewed through a turbulent phase screen," J. Opt. Soc. Am. A **8**, 1142–1147 (1991).
10. G. J. Balmer, D. L. Jordan, P. R. Tapster, M. J. Kent, and E. Jakeman, "Double passage wave propagation effects at infrared and visible frequencies," Opt. Commun. **88**, 6–12 (1992).
11. J. W. Goodman, "Statistical properties of speckle patterns," in *Laser Speckle and Related Phenomena*, 2nd. ed., J. C. Dainty, ed. (Springer-Verlag, Berlin, 1984), pp. 9–75.
12. D. Léger, E. Mathieu, and J. C. Perrin, "Optical surface roughness determination using speckle correlation technique," Appl. Opt. **14**, 872–877 (1975).
13. D. Léger and J. C. Perrin, "Real-time measurement of surface roughness by correlation of speckle patterns," J. Opt. Soc. Am. **66**, 1210–1217 (1976).
14. S. Feng, C. Kane, P. A. Lee, and A. D. Stone, "Correlations and fluctuations of coherent wave transmission through disordered media," Phys. Rev. Lett. **61**, 834–837 (1988).
15. R. Berkovits, M. Kaveh, and S. Feng, "Memory effect of waves in disordered systems: a real-space approach," Phys. Rev. B **40**, 737–740 (1989).
16. S. Feng, "Novel correlations and fluctuations in speckle patterns," in *Scattering and Localization of Classical Waves in Random Media*, P. Sheng, ed. (World Scientific, Singapore, 1990), pp. 179–206.
17. I. Freund and M. Rosenbluh, "Time reversal symmetry of

multiply scattered speckle patterns," Opt. Commun. **82,** 362–366 (1991).
18. C. J. R. Sheppard and T. Wilson, "Image formation in scanning microscopes with partially coherent source and detector," Opt. Acta **25,** 315–325 (1978).
19. E. Jakeman and J. G. McWhirter, "Correlation function dependence on the scintillation behind a deep random phase screen," J. Phys. A **10,** 1599–1643 (1977).
20. I. S. Reed, "On a moment theorem for complex Gaussian processes," IRE Trans. Inf. Theory **IT-8,** 194–195 (1962).
21. M. P. Van Albada and A. Lagendijk, "Observation of weak localization of light in a random medium," Phys. Rev. Lett. **55,** 2692–2695 (1985).
22. P. E. Wolf and G. Maret, "Weak localization and coherent backscattering of photons in disordered media," Phys. Rev. Lett. **55,** 2696–2699 (1985).
23. A. Ishimaru, "Experimental and theoretical studies of enhanced backscattering from scatterers and rough surfaces," in *Scattering in Volumes and Surfaces,* M. Nieto-Vesperinas and J. C. Dainty, eds. (North-Holland, Amsterdam, 1990), pp. 1–15.
24. I. Freund, M. Rosenbluh, and R. Berkovits, "Geometric scaling of the optical memory effect in coherent-wave propagation through random media," Phys. Rev. B **39,** 12403–12406 (1989).
25. P. Beckmann and A. Spizzichino, *The Scattering of Electromagnetic Waves from Rough Surfaces* (Pergamon, Oxford, 1963), pp. 85–87.